Beam and hot-spot formation in a low impedance line driven vacuum spark discharge

E. Wyndham, H. Chuaqui, M. Favre, L. Soto, and P. Choi

Citation: Journal of Applied Physics **71**, 4164 (1992); doi: 10.1063/1.350819
View online: https://doi.org/10.1063/1.350819
View Table of Contents: http://aip.scitation.org/toc/jap/71/9
Published by the American Institute of Physics

Beam and hot-spot formation in a low impedance line driven vacuum spark discharge

E. Wyndham, H. Chuaqui, M. Favre, and L. Soto
Facultad de Fisica, Pontificia Universidad Católica de Chile, Casilla 306, Santiago 22, Chile

P. Choi
The Blackett Laboratory, Imperial College, London SW7 2BZ, United Kingdom

(Received 16 October 1991; accepted for publication 21 January 1992)

Observations of a vacuum spark discharge are presented using a coaxial line driver. A 120 ns, 1.5 Ω coaxial line is used to give peak discharges of 90 kA. The usual line spark gap is shorted out giving a new mode of operation. The discharge is initiated once the rising sinusoidal voltage is applied by focusing a Nd:YAG laser onto the cathode front surface, peak current is reached at 250 ns after this. Reproducible hot spot formation is observed at this time. Holographic interferometry combined with time and space resolved x-ray observations show emission from a dense anode plasma as well as from the dense plasma column in which hot spot forms at peak current.

INTRODUCTION

The vacuum spark has been a fruitful subject of experimental and theoretical research for over two decades, and extensive reviews are available[1,2] which give a full discussion of various mechanisms associated with the formation of electron beams and plasmas in which radiative collapse is observed. The great majority of experimental results have been obtained using low inductance capacitor bank circuits allowing dI/dt of order 2×10^{11} A s^{-1}. Fewer results have been presented[3] when using a low impedance switched coaxial line as the driver, where dI/dt values are much higher. Although the typical peak currents are lower for a given charging voltage, such generators have the characteristic that on the time scale of the current disruptions associated with the time scales of plasma point formation the source impedance is substantially less than the traditional arrangement, as the inductive component is greatly reduced.

In this paper we present the first results of a third or "hybrid" regime of operation of the vacuum spark which is a hybrid of the above options. Here a coaxial line is used but the voltage is allowed to build up slowly and sinusoidally until the discharge is initiated by a laser pulse. During the conduction phase the discharge is driven by the coaxial line resulting in a higher value of dI/dt of 8×10^{11} A s^{-1}, which is an intermediate value when compared with a typical value of dI/dt of order 2×10^{12} A s^{-1} of a switched coaxial line generator.

Chains of hot spots are observed with a repeatable spatial distribution at the time of peak current. The x-ray emission was resolved both in energy and its evolution was spatially and temporally resolved. A sequence of holographic interferograms shows the development of several pinch plasmas of different characteristics during the time to peak current. First a broad and expanding plasma channel is seen during current buildup, which on breaking up, gives rise to a second dense plasma column close to the cathode in which the hot spots are formed. The electron density of the plasma column is measured and the temperature of the hot spots may be estimated from the x-ray information.

APPARATUS

The voltage driver consists of a 400 kV, 25 nF Marx generator operated at 450 J stored energy coupled to a coaxial line whose double transit time is 120 ns and impedance is 1.5 Ω.[4] The conical anode has a 2.5 mm perforation which allows the laser light to be focused at normal incidence onto the cathode front surface. The cathode has a slight axial recess of 1.5 mm deep and 3 mm diameter. An anode-cathode separation of 8 mm was found to be optimum for hot spot formation. The electrode material was copper. The initiating laser pulse was from a Q-switched Nd:YAG laser giving 0.4 J in a 40 ns pulse focused at $f/7$. Frequency doubled light, suitably delayed from the same laser was used for the holographic interferometry.

The x-ray diagnostics used were as follows: the time integrated emission was observed with a pinhole camera, using filters of 5 μm Al with 5 μm Mylar. The time-resolved emission was obtained in two ways: first an array of PIN diodes with different filters observed all or part of the emitting regions. Second, spatial and temporal resolution of the x-ray emission was obtained by replacing the film on the pinhole camera with a 0.5-mm-thick disk of Pilot u scintillator and then scanning the emission with a light fiber in contact with the surface, allowing the emission from a core of plasma with a diameter of 1.5 mm to be observed.

EXPERIMENTAL RESULTS

Figure 1 shows typical voltage and current waveforms encountered in the discharge as well as broadband x-ray emission from the whole volume. The voltage is allowed to rise across the electrodes, by shorting the coaxial line spark gap, for 300 ns before the laser is applied. An appreciable current begins (>5 kA) 120 ns after the laser pulse and

 0021-8979/92/094164-04$04.00

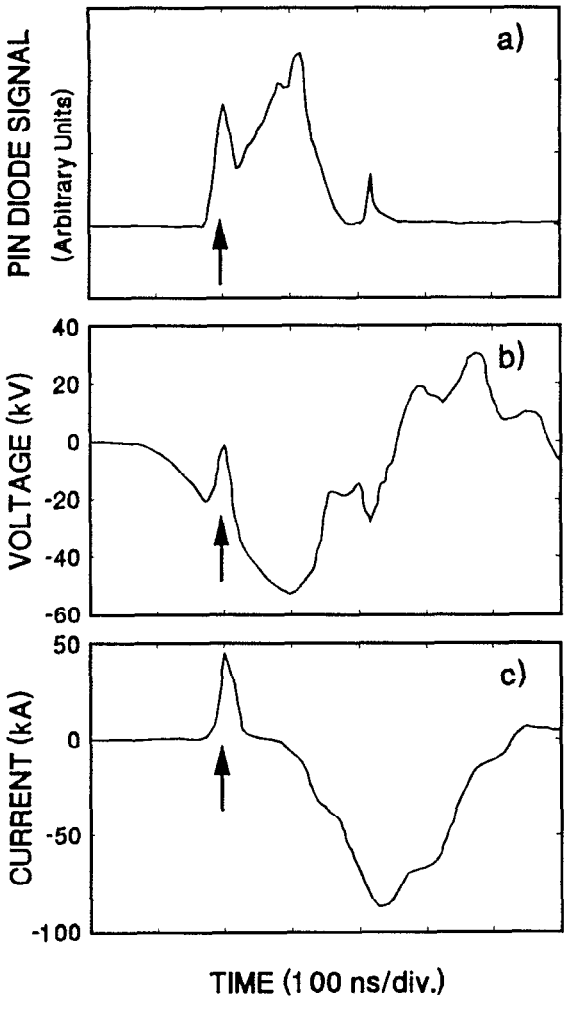

FIG. 1. Broadband x-ray emission from whole discharge, applied voltage measured close to cathode (anode at ground), and discharge current. The arrow indicates the time of the laser pulse, which is superimposed on all traces.

within a further 120 ns peak current is reached. X-ray emission starts as soon as the laser pulse arrives, this is beam target emission from the anode due to electrons accelerated from the laser produced plasma on the cathode surface. As soon as a plasma forms in the interelectrode volume an appreciable current flows and the voltage drops reducing the high energy x-ray content. At a later time close to peak current, a second smaller emission maximum is seen; these x rays are predominantly of the energy band of the copper K_α emission from the anode as well as softer emission from the interelectrode plasma.

A series of measurements of x rays of less than 12 Å is shown as a function of position and time in Fig. 2. For x rays of greater than 50 keV, however, there is no spatial resolution, so a signal of the anode emission is seen at all positions. This last signal ends between 120 and 150 ns after the laser pulse, and the diagnostic from then on allows spatial resolution.

There are considerable differences in x-rays emission at different axial positions after 150 ns. It can be seen that from the cathode to 2 mm from the anode there is no

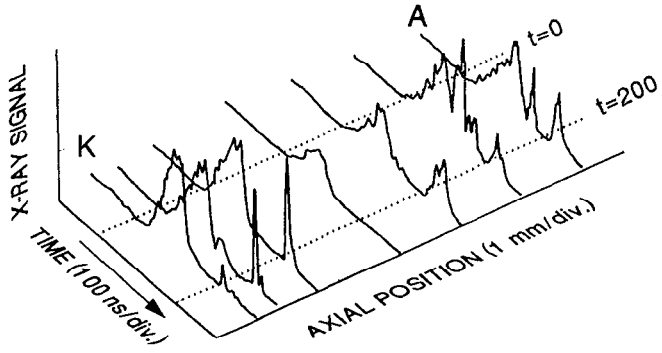

FIG. 2. Broadband x-ray emission at a series of positions between the cathode (K) and the anode (A).

emission until the time of 220 ns other than hard x-ray emission as stated above. At and near the anode we find emission up to 200 ns, after which there is no emission until just before peak current. At this time we observe a short 6–8 ns full width half maximum (FWHM) pulse in the interelectrode region at between 1 and 3.5 mm from the cathode. The emission from the cathode also shows this feature but of smaller amplitude. The emission from the anode shows a broader 30 ns pulse. The plasma emission at 1.5 mm from the anode shows the short pulse superimposed on a broader pulse. The precise relative timing could not be established as each trace corresponds to a different shot. The short pulse seen close to the cathode clearly coincides with the hot spot emitting region as may be seen from Fig. 3, which shows a time integrated pinhole photograph using the same filtering. It can be seen that several hot spots form within the 8 ns pulse.

The energy of the x-ray emission was studied using filters 5, 10, and 15 μm Al and also 2.5 μm of copper. The effect of using thicker aluminum was to reduce progressively the signal from the hot spot emitting region without altering the emission from the anode and the plasma close to it. When 2.5 μm of Cu was used as the filter material the emission from the hot spot region disappeared but the anode plasma remained without change. The relative attenuation measured in this way allows a first estimate of the hot spot temperature assuming thermal inverse Bremmstrahlung emission of approximately 800 eV. The emission from the anode plasma from this and other measurements is predominantly between 1 and 5 Å. No high energy x-ray component is seen at this time.

It is of great importance to know the electron density distribution and for this purpose a series of holographic interferograms was taken. In Fig. 4 a sequence of holograms was taken at 532 nm at times between 190 and 260 ns after the maximum of the laser initiation pulse. The effective exposure time of 20 ns is rather long compared to some of the fluid movement time scales. Before 170 ns there are no observable fringe shifts to be seen. However within the 70 ns following the first of the four interferograms shown, two separate plasma columns are formed. The first column is observed at 190 ns after the initiating pulse and is rather irregular with a diameter of 2–3 mm

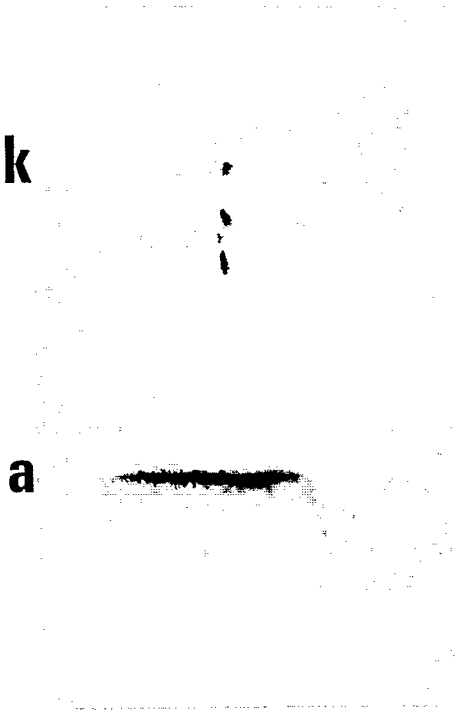

FIG. 3. Time integrated image of the broadband x-ray emission.

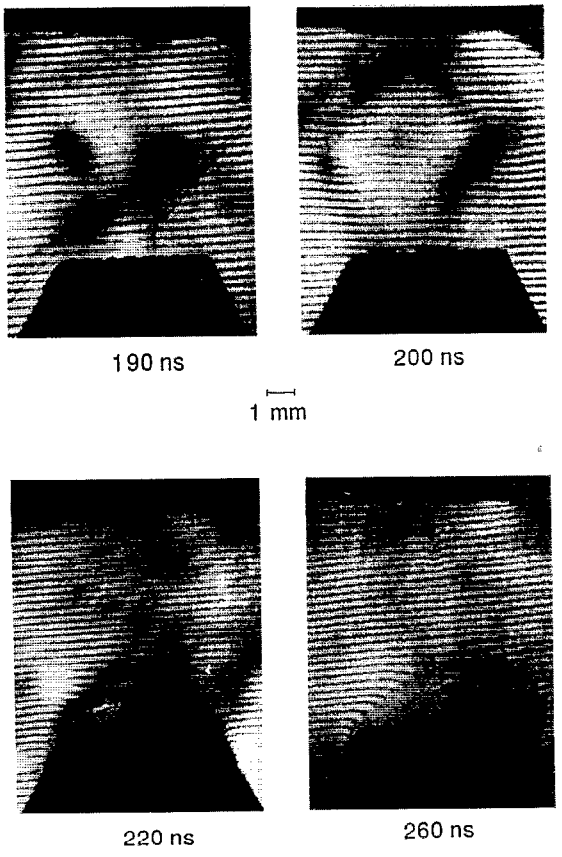

FIG. 4. A series of holographic interferograms of the vacuum spark in hybrid mode taken in the run up to peak current at 260 ns after the initiating laser pulse.

and with $N_e \sim 2 \times 10^{18}$ cm^{-3}. This channel is seen to expand rapidly and breaks up so that at 220 ns occupies a diameter of 1.5 cm. The breakup coincides with a large drop in the current signal. At this time a plasma is seen to form on the anode and propagate towards the cathode occupying some 2 or 3 mm of the channel by 260 ns. At 260 ns the formation of a narrow plasma column less than 1 mm in diameter with $N_e \sim 10^{19}$ cm^{-3} is seen near the cathode. This corresponds both to the position of hot spot formation seen in the pinhole photographs as well as the pulses seen at this time and position from the scintillator. The laser pulse is long compared to the characteristic hot spot emission durations, so resolution of individual hot spots is not expected.

DISCUSSION

The results indicate that the generator parameters used in this experiment are suitable for the formation of hot spots. There are similarities with the observations seen when using a switched coaxial line,[3] where a rather larger plasma column is associated with hot spot formation. In that case an optimum anode cathode separation of some 3 mm was found, whereas in this situation no hot spots were seen at this separation. For such short separations in the hybrid mode of operation, self breakdown occurs before the laser pulse arrives giving rise to much lower values of peak current.

Comparison with interferometry done in a traditional discharge[5] shows that the electronic density here is lower until the second or narrow plasma column is observed. Shadowgraphy of traditional discharges do show a narrow plasma column,[6] but positioned in the middle of the discharge. In such a discharge with laser initiation the hot spots are seen close to the anode and not near the cathode as reported here.

The laser powers used in this experiment are considerably lower than those used both in switched line driven and in traditional vacuum spark discharges.[7] However, a high degree of reproducibility was observed here in keeping with other work using laser initiation. In our present work we found a threshold of 200 mJ for hot spot formation. At energies below this the electrical behavior of the breakdown was similar but only intense x-ray emission from the anode was seen; no hot spots were found even though peak currents were approximately the same.

It appears that the disruption of the first (wide) plasma channel is associated with an enhanced anode x-ray emission which coincides with the plasma seen evolving from the anode surface in the interferograms. From this observation we may infer the presence of intense electron beams at this time. During hot spot emission a shorter anode pulse is also seen superposed on the anode plasma formed in the previous 40 ns indicative of enhanced electron beam generation in this period. This can be associated

with self-pinching of the narrow plasma column where hot spots are formed.

If the discharge was operated at lower charging voltage so that peak currents are slightly below 50–60 kA no hot spots can be observed. This threshold for the formation of hot spots is a little below the theoretical estimate given in Ref. 8 taking $T \sim 1$ keV and $Z \sim 20$. However, the hot spot temperature seen here is rather lower than that seen in generators with a higher peak current ($\geqslant 100$ kA), suggesting that 90 kA is barely sufficient to induce complete radiative collapse.

The exact relative timing of the pulse of x rays from the various points in the plasma has yet to be determined, however the indication is that they are within a few ns of each other.

It is noteworthy that in this experiment the hot spots are formed in a plasma channel close to the cathode and not in the plasma formed close to the anode by electron beam bombardment. The reproducible nature of their position may be due to the fact that they are formed elsewhere from the anode plasma, which is seen to have a considerable shot-to-shot variation in its distribution.

In conclusion, we have presented a new regime of vacuum spark operation where hot spots are formed in a column of plasma close to the cathode. The formation and evolution of the plasma electron density and temperature has been discussed showing clear differences between the different characteristic plasmas.

We would like to acknowledge with gratitude the support of FONDECYT and Fundación Andes. L. Soto has a fellowship with Fundación Andes.

[1] E. D. Korop, B. E. Meierovich, Yu. V. Sidelnikov, and S. T. Sukhorukov, Sov. Phys. Usp. **22**, 727 (1979).
[2] K. N. Koshelev and N. R. Pereira, J. Appl. Phys. **69**, R21 (1991).
[3] S. M. Zakharov, G. V. Ivanenkov, A. a. Kolomenskii, S. A. Pikuz, and A. I. Samokhin, Sov. Tech. Phys. Lett. **8**, 155 (1982).
[4] M. Favre, in "Pulse technology: Pulsed power for pinch research," *Small Plasma Physics Experiments II*, edited by S. Lee and P. H. Sakanaka (World Scientific, Singapore, 1990), p. 170.
[5] C. R. Negus and N. J. Peacock, J. Phys. D: Appl. Phys. **12**, 91 (1979).
[6] V. A. Veretennikov, V. A. Gribkov, E. Ya. Kononov, O. G. Semenov, and Yu. V. Sidel'nikov, Sov. J. Plasma Phys. **7**, 249 (1981).
[7] C. S. Wong and S. Lee, Rev. Sci. Instrum. **55**, 1125 (1984).
[8] P. S. Antsiferov, K. N. Koshelev, A. E. Kramida, and A. M. Panin, J. Phys. D: Appl. Phys. **22**, 1073 (1989).